

Preparation, characterization and magnetic behavior of a spin-labelled physical hydrogel containing a chiral cyclic nitroxide radical unit fixed inside the gelator molecule

Yusa Takemoto,¹ Takayuki Yamamoto,¹ Naohiko Ikuma,² Yoshiaki Uchida,^{3,4} Katsuaki Suzuki,¹ Satoshi Shimono,¹ Hiroki Takahashi,¹ Nobuhiro Sato,⁵ Yojiro Oba,⁵ Rintaro Inoue,⁵ Masaaki Sugiyama,⁵ Hirohito Tsue,¹ Tatsuhisa Kato,¹ Jun Yamauchi,¹ Rui Tamura*¹

¹Graduate School of Human and Environmental Studies, Kyoto University, Kyoto 606-8501, Japan

²Graduate School of Engineering, Osaka University, Suita, Osaka 565-0871, Japan

³Graduate School of Engineering Science, Osaka University, Toyonaka, Osaka 560-8531, Japan

⁴Japan Science and Technology Agency, PRESTO, 4-1-8 Honcho, Kawaguchi, Saitama 332-0012, Japan

⁵Research Reactor Institute, Kyoto University, Osaka 590-0494, Japan

Supporting Information

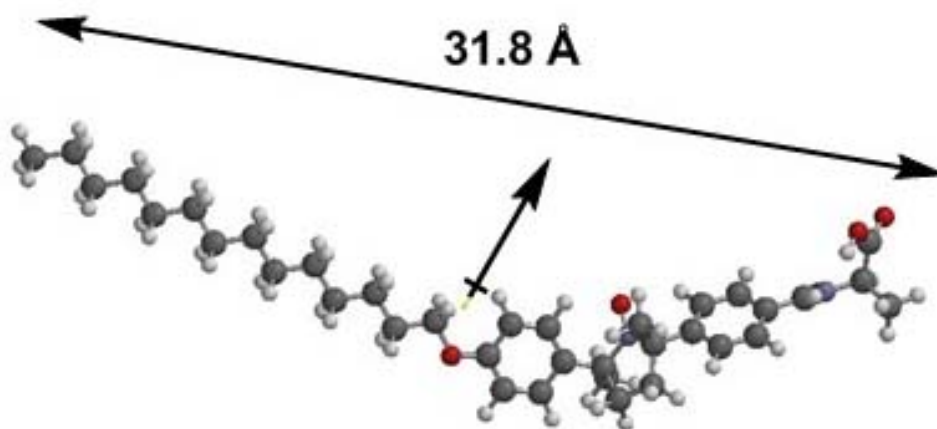
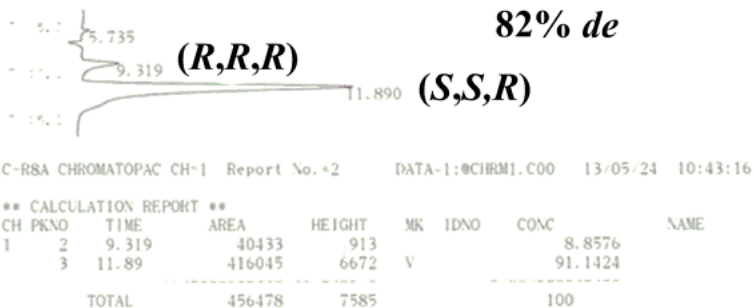
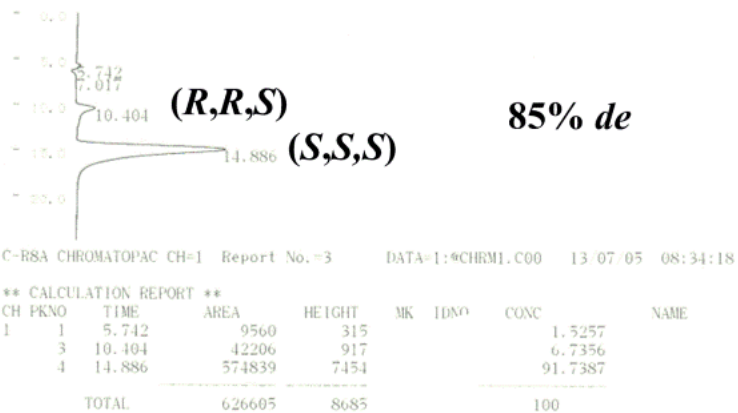


Fig. S1 The molecular conformation of (*S,S,R*)-5a optimized by AM1 method (PC Spartan'02) of the virtual molecule (*S,S,R*)-5a derived from the crystal structure of (*S,S,S*)-5b (Figure 4). The arrow indicates the direction of molecular polarization.

(a)



(b)



(c)

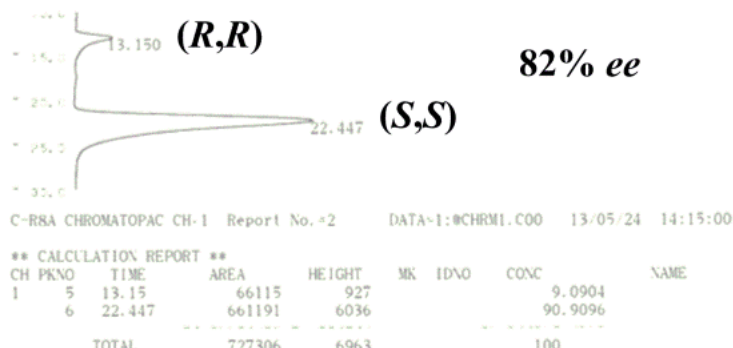


Fig. S2 HPLC chromatograms. (a) (*S,S,R*)-**5a** of 82% *de*, (b) (*S,S,S*)-**5b** of 85% *de*, and (c) (*S,S*)-**5c** of 82% *ee*. HPLC analysis was carried out using a chiral stationary phase column (Daicel Chiralpak OD-H, 0.46 cm × 25 cm) at 30 °C, a mixture of hexane, 2-Propanol and TFA (700:300:5) as the mobile phase at the flow rate of 0.5 mL/min and a UV-vis spectrometer (254 nm) as the detector.

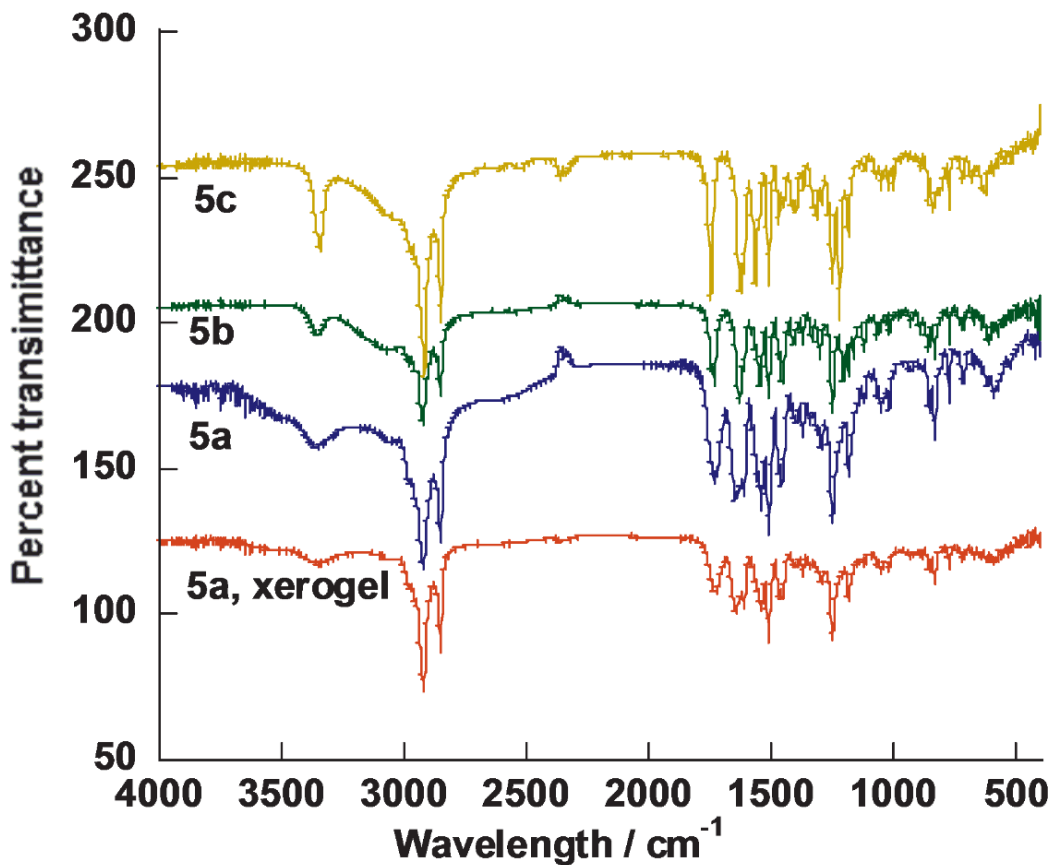


Fig. S3 IR spectra of the xerogel (red) and powder (blue) samples of (*S,S,R*)-**5a**, the powder samples of (*S,S,S*)-**5b** (green) and (*S,S*)-**5c** (yellow) dispersed in a KBr pellet.

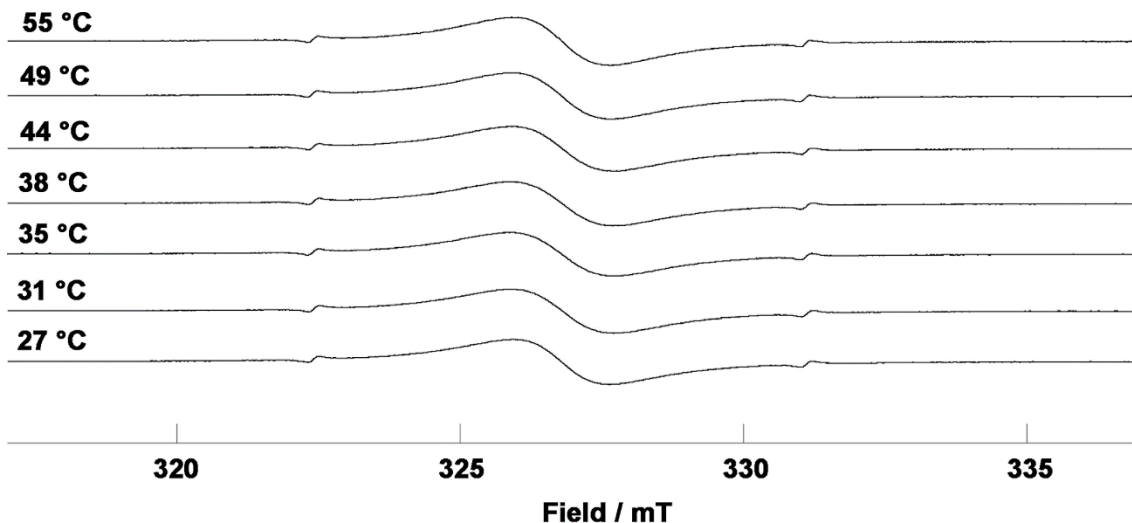


Fig. S4 Selected EPR spectra of the hydrogel and sol of (*S,S,R*)-**5a** measured at various temperatures in the cooling run.

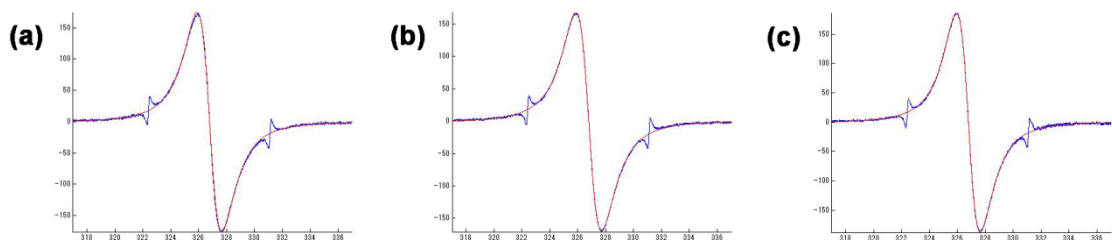


Fig. S5 Observed EPR spectra (blue) and the simulation spectra (red) of (*S,S,R*)-**5a** in the first cooling run used for the determination of the *g*-value; (a) in the hydrogel at 27 °C, (b) in the sol at 35 °C, and (c) in the sol at 55 °C.

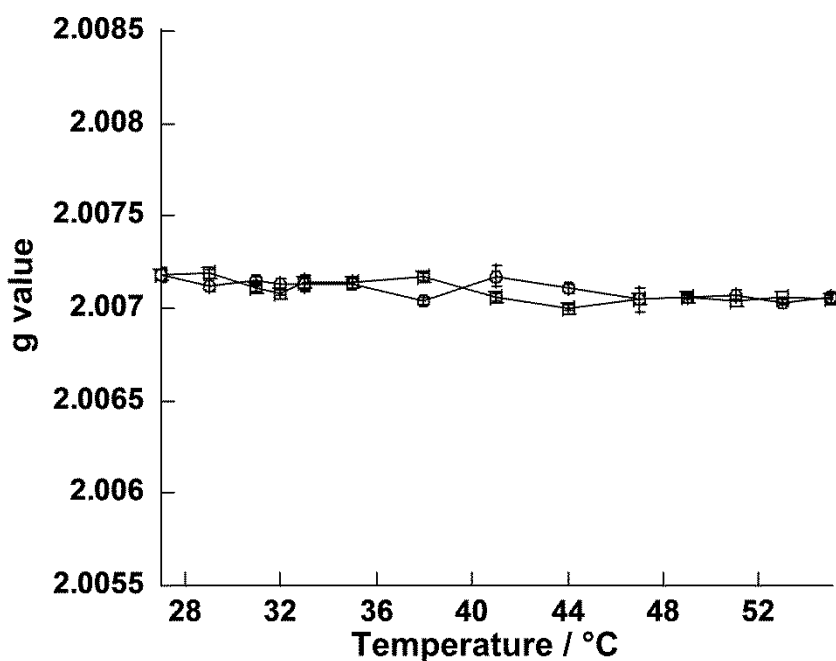


Fig. S6 Temperature dependence of g-value in the gel and sol states of (*S,S,R*)-**5a** by EPR spectroscopic studies. Circles denote the first cooling run, while squares represent the second heating run.

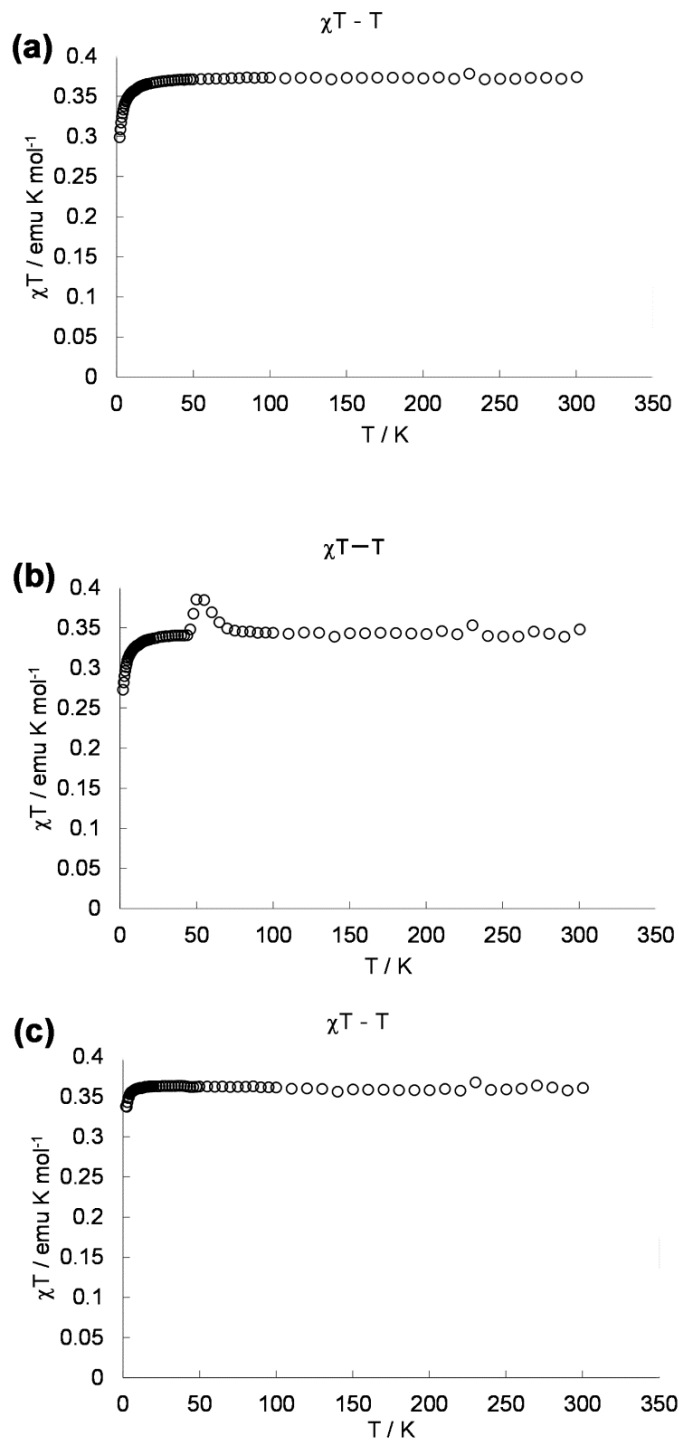


Fig. S7 Temperature dependence of molar magnetic susceptibilities at 0.05 T in the temperature ranges of 2-300 K in the first heating run by SQUID measurements. (a) Powder sample and (b) xerogel of (S,S,R) -**5a**, and (c) powder sample of (S,S,S) -**5b**. Oxygen gas could not be removed completely from the xerogel by repeated evacuation as seen in panel (b).

Table S1 Results of EPR spectral simulation to determine the *g*-value with rmsd for the hydrogel and sol of (*S,S,R*)-**5a** in the first cooling and second heating runs.

Cooling					
Temperature (°C)	g-value (hydrogel & sol)			Average	Standard deviation
	1	2	3		
27	2.007	2.007	2.007	2.007	0
29	2.007	2.007	2.007	2.007	0
31	2.007	2.007	2.007	2.007	0
32	2.007	2.007	2.007	2.007	0
33	2.007	2.007	2.007	2.007	0
35	2.007	2.007	2.007	2.007	0
38	2.007	2.007	2.007	2.007	0
41	2.007	2.007	2.007	2.007	0
44	2.007	2.007	2.007	2.007	0
47	2.007	2.007	2.007	2.007	0
49	2.007	2.007	2.007	2.007	0
51	2.007	2.007	2.007	2.007	0
53	2.007	2.007	2.007	2.007	0
55	2.007	2.007	2.007	2.007	0

Heating					
Temperature (°C)	g-value (hydrogel & sol)			average	Standard deviation
	1	2	3		
27	2.007	2.007	2.007	2.007	0
29	2.007	2.007	2.007	2.007	0
31	2.007	2.007	2.007	2.007	0
32	2.007	2.007	2.007	2.007	0
33	2.007	2.007	2.007	2.007	0
35	2.007	2.007	2.007	2.007	0
38	2.007	2.007	2.007	2.007	0
41	2.007	2.007	2.007	2.007	0
44	2.007	2.007	2.007	2.007	0
47	2.007	2.007	2.007	2.007	0
49	2.007	2.007	2.007	2.007	0

51	2.007	2.007	2.007	2.007	0
53	2.007	2.007	2.007	2.007	0
55	2.007	2.007	2.007	2.007	0

Cooling					
Temperature (°C)	Rmsd (hydrogel & sol)			average	Standard deviation
	1	2	3		
27	0.025	0.025	0.025	0.025	0.000
29	0.025	0.025	0.026	0.025	0.000
31	0.025	0.026	0.025	0.025	0.000
32	0.025	0.025	0.025	0.025	0.000
33	0.025	0.025	0.025	0.025	0.000
35	0.025	0.025	0.025	0.025	0.000
38	0.025	0.025	0.025	0.025	0.000
41	0.024	0.025	0.025	0.025	0.000
44	0.024	0.025	0.024	0.025	0.000
47	0.024	0.024	0.024	0.024	0.000
49	0.024	0.024	0.024	0.024	0.000
51	0.024	0.025	0.023	0.024	0.001
53	0.024	0.024	0.024	0.024	0.000
55	0.024	0.023	0.024	0.023	0.000

Heating					
Temperature (°C)	Rmsd (hydrogel & sol)			average	Standard deviation
	1	2	3		
27	0.025	0.025	0.025	0.025	0.000
29	0.025	0.025	0.025	0.025	0.000
31	0.025	0.025	0.025	0.025	0.000
32	0.025	0.025	0.025	0.025	0.000
33	0.025	0.025	0.025	0.025	0.000
35	0.025	0.025	0.025	0.025	0.000
38	0.025	0.025	0.025	0.025	0.000
41	0.025	0.025	0.025	0.025	0.000
44	0.025	0.025	0.025	0.025	0.000

47	0.025	0.025	0.025	0.025	0.000
49	0.025	0.024	0.025	0.025	0.000
51	0.025	0.024	0.025	0.025	0.000
53	0.024	0.024	0.024	0.024	0.000
55	0.024	0.024	0.024	0.024	0.000

Table S2 Curie constant and Weiss constant of powder sample and xerogel of (*S,S,R*)-**5a**, and powder sample of (*S,S,S*)-**5b** by SQUID measurements.

	Curie constant (emu K mol ⁻¹)	Weiss constant (K)
Powder, (<i>S,S,R</i>)- 5a	0.37	-0.39
Xerogel, (<i>S,S,R</i>)- 5a	0.34	-0.28
Powder, (<i>S,S,S</i>)- 5b	0.36	-0.17